

Phase transition in compressible Ising systems at fixed volume

Akira Onuki and Akihiko Minami

Department of Physics, Kyoto University, Kyoto 606-8502, Japan

(Dated: February 1, 2008)

Using a Ginzburg-Landau model, we study the phase transition behavior of compressible Ising systems at constant volume by varying the temperature T and the applied magnetic field h . We show that two phases can coexist macroscopically in equilibrium within a closed region in the T - h plane. Its occurrence is favored near tricriticality. We find a field-induced critical point, where the correlation length diverges, the difference of the coexisting two phases and the surface tension vanish, but the isothermal magnetic susceptibility does not diverge in the mean field theory. We also investigate phase ordering numerically.

PACS numbers: 75.30.Kz, 62.20.Dc, 64.60.Kw, 05.70.Fh

I. INTRODUCTION

Solids are under the influence of elastic constraints and their phase transitions are often decisively influenced by couplings of the order parameter and the elastic field¹. Such elastic effects strongly depend on the nature of the coupling and their understanding is crucial in technology. In the present work, we will focus on the phase transition behavior of compressible ferromagnets or antiferromagnets, which has long been studied theoretically in the physics community^{2,3,4,5,6,7,8,9,10,11,12}. In real materials, the short-range spin interactions depend on the distances among the spins, so the spin fluctuations are coupled to the elastic dilation strain. In the literature on this problem, the main issue has been the effect of the elastic coupling on the critical behavior of the spin system. A remarkable but subtle result of the renormalization group calculations^{8,9} is that the cubic elastic anisotropy becomes increasingly important on approaching the critical point (which is determined in the absence of the anisotropy). This renormalization effect should trigger a first order phase transition sufficiently close to the critical point. Simulations have been performed on compressible Ising systems and a number of numerical results still remain not well understood^{10,11,12}. These theories and simulations show that the phase transition depends on whether the pressure or the volume is fixed.

In this paper, we will present a mean field theory of compressible Ising systems at constant volume using a Ginzburg-Landau free energy. Our main objectives are to demonstrate the presence of unique two phase coexistence near the tricritical point and to examine phase ordering after changing the temperature. Though our theory is a rough approximation, it will provide overall phase behavior for general values of the parameters.

The organization of this paper is as follows. In Sec. II, we will present a model, in which the order parameter and the elastic field are coupled, and eliminate the elastic degrees of freedom assuming the mechanical equilibrium condition. In Sec. III, we will examine the phase behavior in the plane of the temperature T and the ordering field h . Detailed calculations will also be given on the susceptibility, the correlation length, and the surface ten-

sion. The presence of a unique field-induced critical point will also be reported. In Sec. IV, we will numerically integrate the time-dependent Ginzburg-Landau equation in two dimensions (2D). In the appendix, we will derive the free energy at constant pressure (or applied stress), where two-phase coexistence can be realized only on lines in the T - h plane.

II. THEORETICAL BACKGROUND

A. Ginzburg-Landau free energy

We assume that a single-component order parameter ψ is coupled to the elastic displacement \mathbf{u} . We set up the Ginzburg-Landau free energy functional $F = F\{\psi, \mathbf{u}\}$ in the form¹³,

$$F = \int d\mathbf{r} \left[f_0 + \frac{C}{2} |\nabla \psi|^2 + \alpha \psi^2 e_1 + f_{el} \right], \quad (2.1)$$

where the space integral is within the system with volume V . The first part $f_0 = f_0(\psi)$ depends on ψ as

$$f_0 = \frac{\tau}{2} \psi^2 + \frac{\bar{u}}{4} \psi^4 + \frac{v}{6} \psi^6 - h \psi. \quad (2.2)$$

The coefficient τ depends on the temperature T as

$$\tau = A_0(T - T_0), \quad (2.3)$$

where A_0 is a positive constant and T_0 is the critical temperature in the absence of the elastic coupling. The other coefficients are treated to be independent of T . We fix the other field variables such as the hydrostatic pressure. The coefficients v and C are positive, while \bar{u} can be either positive or negative. The h represents a magnetic or electric field conjugate to ψ . For antiferromagnetic materials, no uniform field conjugate to the antiferromagnetic order can be realized, so $h = 0$. We may assume $h \geq 0$ without loss of generality. If $h = 0$, F is invariant with respect to $\psi \rightarrow -\psi$. The α represents the strength of the coupling between ψ^2 and the dilation strain,

$$e_1 = \nabla \cdot \mathbf{u}. \quad (2.4)$$

This coupling arises when the interaction among the fluctuations of ψ depends on the local lattice expansion or contraction.

In cubic crystals, the elastic energy density is of the form,

$$f_{\text{el}} = \frac{C_{11}}{2} \sum_i \epsilon_{ii}^2 + \sum_{i \neq j} \left[\frac{C_{12}}{2} \epsilon_{ii} \epsilon_{jj} + C_{44} \epsilon_{ij}^2 \right], \quad (2.5)$$

where C_{11} , C_{12} , and C_{44} are the usual elastic moduli assumed to be constant, and $\epsilon_{ij} = (\nabla_i u_j + \nabla_j u_i)/2$ is the symmetrized strain tensor. The dependence of the elastic moduli on ψ^2 can be important at low temperatures, however. Hereafter $\nabla_i = \partial/\partial x_i$. The elastic stress tensor σ_{ij} is expressed as

$$\begin{aligned} \sigma_{ii} &= (C_{11} - C_{12})\epsilon_{ii} + C_{12}e_1 + \alpha\psi^2, \\ \sigma_{ij} &= 2C_{44}\epsilon_{ij} \quad (i \neq j). \end{aligned} \quad (2.6)$$

Nonvanishing ψ^2 gives rise to a change in the diagonal stress components. We then obtain $\sum_j \nabla_j \sigma_{ij} = -\delta F/\delta u_i$, where ψ is fixed in the functional derivative of F with respect to u_i . Note that a constant hydrostatic pressure p_0 can be present in the reference state, where the total stress tensor is $p_0\delta_{ij} - \sigma_{ij}$.

B. Elimination of elastic field at fixed volume

The elastic field \mathbf{u} is determined by ψ under the mechanical equilibrium condition,

$$\sum_j \nabla_j \sigma_{ij} = 0. \quad (2.7)$$

Furthermore, in this paper, we impose the periodic boundary condition on δu in the region $0 < x, y, z < V^{1/d}$. This can be justified when the solid boundary is mechanically clamped. See Appendix A for the case of fixed applied pressure. The space averages of the strains then vanish; for example, $\langle e_1 \rangle = 0$. Hereafter $\langle \dots \rangle = \int d\mathbf{r}(\dots)/V$. The following procedure of eliminating the elastic field has been derived by many authors in the literature in physics and engineering^{1,2,4,5,11,14}.

It is convenient to use the Fourier transformation, $u_j(\mathbf{r}) = \sum_{\mathbf{k}} u_{j\mathbf{k}} \exp(i\mathbf{k} \cdot \mathbf{r})$, where \mathbf{k} is the wave vector. Then the Fourier component of e_1 is expressed as

$$e_{1\mathbf{k}} = -\alpha\varphi_{\mathbf{k}}/[C_{12} + C_{44} + C_{44}\zeta(\hat{\mathbf{k}})], \quad (2.8)$$

where $\varphi_{\mathbf{k}}$ is the Fourier component of the variable,

$$\varphi(\mathbf{r}) = \psi^2 - \langle \psi^2 \rangle. \quad (2.9)$$

The space average of φ is made to vanish. The $\zeta(\hat{\mathbf{k}})$ is a function of the direction of the wave vector $\hat{\mathbf{k}} = k^{-1}\mathbf{k}$ and is defined by

$$\zeta(\hat{\mathbf{k}})^{-1} = \sum_j \hat{k}_j^2 / (1 + \xi_a \hat{k}_j^2), \quad (2.10)$$

where ξ_a is the degree of cubic anisotropy,

$$\xi_a = (C_{11} - C_{12})/C_{44} - 2. \quad (2.11)$$

We have $\zeta(\hat{\mathbf{k}}) = 1$ in the isotropic elasticity $\xi_a = 0$. After some calculations, we may eliminate \mathbf{u} in F to obtain the free energy $F = F\{\psi\}$ of ψ only in the form¹,

$$F = \int d\mathbf{r} \left[f_0 + \frac{C}{2} |\nabla\psi|^2 \right] - \frac{1}{2V} \sum_{\mathbf{k}} w(\hat{\mathbf{k}}) |\varphi_{\mathbf{k}}|^2. \quad (2.12)$$

The second term on the right hand side arises from the elastic coupling and is negative, where

$$w(\hat{\mathbf{k}}) = \alpha^2/[C_{12} + C_{44} + C_{44}\zeta(\hat{\mathbf{k}})]. \quad (2.13)$$

The functional derivative of F is performed to give

$$\frac{\delta F}{\delta \psi} = f'_0 - C\nabla^2\psi + 2\alpha e_1\psi, \quad (2.14)$$

where $f'_0 = \partial f_0/\partial \psi$ and the Fourier transformation of e_1 is in Eq.(2.8). In equilibrium we require $\delta F/\delta \psi = 0$.

We further simplify our free energy. In the isotropic elasticity, $w(\hat{\mathbf{k}})$ is a constant independent of $\hat{\mathbf{k}}$ and $e_1 = -\alpha\varphi/C_{11}$. Then F is rewritten as

$$F = \int d\mathbf{r} \left[f_0 + \frac{C}{2} |\nabla\psi|^2 - \frac{\beta}{4} (\psi^2 - \langle \psi^2 \rangle)^2 \right], \quad (2.15)$$

where φ is explicitly written in terms of ψ and β is a positive constant defined by

$$\beta = 2\alpha^2/C_{11}. \quad (2.16)$$

The presence of the space average $\langle \psi^2 \rangle$ is a unique aspect arising from elasticity.

In cubic solids with $\xi_a < 0$, $w(\hat{\mathbf{k}})$ is maximized along one of the principal crystal axes (say, along the [100] direction in 3D)¹. If $\xi_a > 0$, it is maximized for $\hat{k}_j^2 = 1/d$ for all j (say, along [111] in 3D). Let w_M be the maximum of $w(\hat{\mathbf{k}})$ attained along these soft directions; then,

$$\begin{aligned} w_M &= \alpha^2/C_{11} \quad (\xi_a < 0), \\ &= \alpha^2/[K + (2 - 2/d)C_{44}] \quad (\xi_a > 0). \end{aligned} \quad (2.17)$$

where $K = C_{11}/d + C_{12}(1 - 1/d)$ is the bulk modulus. In 2D, $w(\theta) = w(\hat{\mathbf{k}})$ is a periodic function of the angle θ defined by $k_x/k = \cos\theta$ and $k_y/k = \sin\theta$ with period $\pi/2$, as displayed in Fig. 1. In phase ordering processes, the interface normals tend to be parallel to these soft directions, resulting in cuboidal domains^{1,13,15,16}. If the spatial inhomogeneity is mostly along these soft directions except for the edge regions of the domains, the free energy is approximately given by Eq.(2.15) with

$$\beta = 2w_M. \quad (2.18)$$

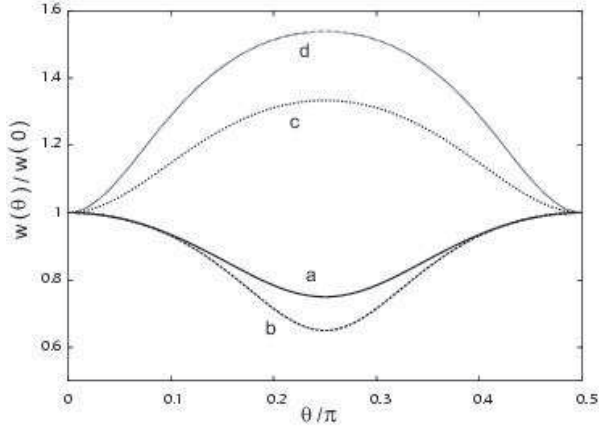


FIG. 1: $w(\theta)/w(0)$ in 2D as a function of θ/π for $((C_{11} - C_{12})/2K, C_{44}/K) = (0.5, 1)$ (a), $(0.3, 1)$ (b), $(1, 0.5)$ (c), and $(1, 0.3)$ (d). The maximum of $w(\theta)$ is $w(0)$ for $\xi_a < 0$ and $w(\pi/2)$ for $\xi_a > 0$.

C. One phase states

We start with the free energy Eq.(2.15). If the system consists of a single ordered phase in equilibrium, we have $\psi^2 = \langle \psi^2 \rangle$ and the homogeneous ψ is determined by

$$f'_0 = (\tau + \bar{u}\psi^2 + v\psi^4)\psi - h = 0, \quad (2.19)$$

where the elastic coupling disappears. The inverse susceptibility $\chi^{-1} = (\partial h / \partial \psi)_\tau$ is given by

$$\chi^{-1} = \partial^2 f_0 / \partial \psi^2 = \tau + 3\bar{u}\psi^2 + 5v\psi^4. \quad (2.20)$$

We may consider the structure factor S_k of the thermal fluctuations of the Fourier component $\psi_{\mathbf{k}}$ in the bulk region. To calculate it, we superimpose plane wave fluctuations of ψ on the homogeneous average. The increase of the free energy in the second order yields S_k in the Ornstein-Zernike form

$$S_k = 1/C(k^2 + \kappa^2), \quad (2.21)$$

where κ is the inverse correlation determined by

$$\begin{aligned} C\kappa^2 &= \partial^2 f_0 / \partial \psi^2 - 3\beta\psi^2 + \beta\langle \psi^2 \rangle \\ &= \tau + (3\bar{u} - 2\beta)\psi^2 + 5v\psi^4. \end{aligned} \quad (2.22)$$

In the second line, we have set $\langle \psi^2 \rangle = \psi^2$ because of the existence of a single phase only. Note that $C\kappa^2$ in the second line of Eq.(2.22) is smaller than χ^{-1} in Eq.(2.20) by $2\beta\psi^2$. In cubic solids, κ represents the inverse correlation length for the fluctuations varying in the softest directions. Let τ take a small negative value at $h = 0$ in the case $\bar{u} > 0$; then, $\psi^2 \cong |\tau|/\bar{u}$ from Eq.(2.19), leading to $C\kappa^2 \cong 2(1 - \beta/\bar{u})|\tau|$ from Eq.(2.22). The positivity of κ^2 is attained only for $\beta < \bar{u}$. Obviously, the disordered phase with $\psi = 0$ is unstable for $\tau < 0$. The ordered phase with $\psi^2 = -\bar{u}/2v + \sqrt{\bar{u}^2/4v^2 - \tau}$ (which

is the solution of Eq.(2.19) at $h = 0$) becomes unstable for $\tau > \tau_{\text{in}}$. In particular, as $h \rightarrow 0$, we find

$$\lim_{h \rightarrow 0} \tau_{\text{in}} = -(\beta^2 - \bar{u}^2)/4v. \quad (2.23)$$

III. TWO PHASE COEXISTENCE

A. Two phase states

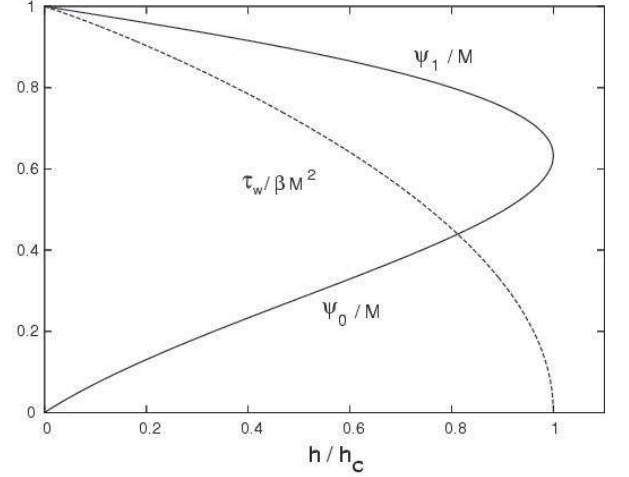


FIG. 2: Normalized order parameters ψ_1/M and ψ_0/M and normalized width of the temperature window $\tau_w/\beta M^2$ versus normalized field h/h_c in two phase coexistence, where M and h_c are defined by (3.9) and (3.12), respectively.

We show that two phases can coexist in a temperature window $\tau_c - \tau_w < \tau < \tau_c$ if the parameter,

$$u = \bar{u} - \beta, \quad (3.1)$$

is negative^{4,5} and h is smaller than a critical field h_c , where τ_c , τ_w , and h_c will be determined below. We of course have $u < 0$ if $\bar{u} < 0$ or if the system undergoes a first order phase transition even without the elastic coupling. For $0 \leq h \leq h_c$ the two phases are characterized by $\psi = \psi_0$ and ψ_1 with $\psi_1 \geq \psi_0 \geq 0$. As $h \rightarrow 0$ we have $\psi_0 \rightarrow 0$, while as $h \rightarrow h_c$ we have $\psi_1 - \psi_0 \rightarrow 0$. We will show that the space average $\langle \psi^2 \rangle$ in the free energy (2.15) gives rise to the two phase coexistence. If it were neglected, we would have the usual tricritical point at $\tau = u = 0$ (see the last paragraph of this subsection)^{1,17}.

If the volume fraction of the phase with $\psi = \psi_1$ is written as ϕ , we have

$$\langle \psi^2 \rangle = \phi\psi_1^2 + (1 - \phi)\psi_0^2. \quad (3.2)$$

The average free energy density $\langle f \rangle = F/V$ is given by

$$\begin{aligned} \langle f \rangle &= \phi f_0(\psi_1) + (1 - \phi)f_0(\psi_0) \\ &\quad + \frac{1}{4}\beta(\psi_1^2 - \psi_0^2)^2(\phi^2 - \phi). \end{aligned} \quad (3.3)$$

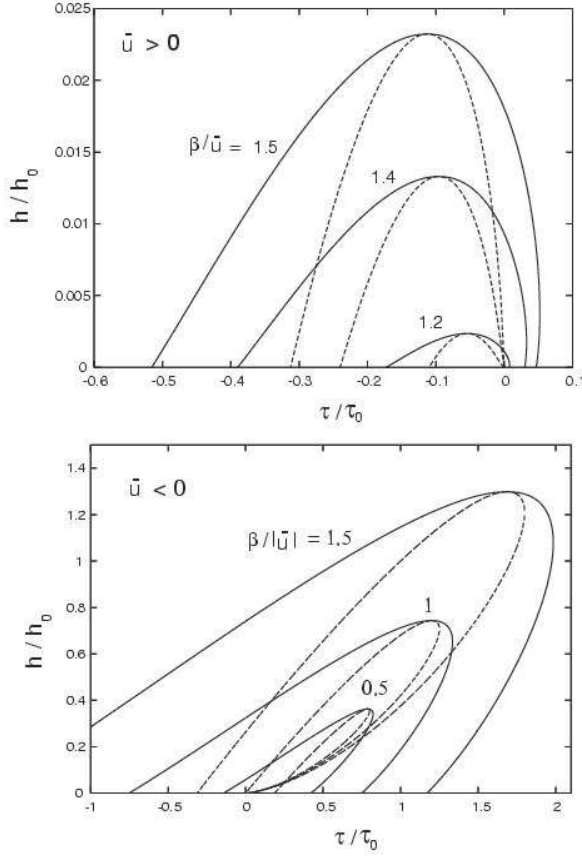


FIG. 3: Phase diagrams in the τ - h plane with $\bar{u} > 0$ for $\beta/\bar{u} = 1.5, 1.4$, and 1.2 (upper plate) and with $\bar{u} < 0$ for $\beta/|\bar{u}| = 1.5, 1$, and 0.5 (lower plate). The τ and h are scaled by $\tau_0 = \bar{u}^2/v$ and $h_0 = v(|\bar{u}|/v)^{5/2} = |6(\beta/\bar{u} - 1)/5|^{5/2} h_c/12$, so h/h_0 is large around $h \sim h_c$ for negative \bar{u} . The system is in two phase coexistence inside each coexistence curve (solid line), while it is in a one phase state outside it. Instability curve (dotted line) merges each coexistence curve at the critical point, inside which one phase states are linearly unstable. @

Here the interface free energy is neglected. The minimization conditions of $\langle f \rangle$ with respect to ψ_1 and ψ_0 are given by

$$f'_0(\psi_1) - \beta(1 - \phi)(\psi_1^2 - \psi_0^2)\psi_1 = 0, \quad (3.4)$$

$$f'_0(\psi_0) + \beta\phi(\psi_1^2 - \psi_0^2)\psi_0 = 0, \quad (3.5)$$

which are equivalent to $\delta F/\delta\psi = 0$ at $\psi = \psi_1$ and ψ_0 . We also minimize $\langle f \rangle$ with respect to ϕ to obtain

$$f_0(\psi_1) - f_0(\psi_0) + \frac{\beta}{4}(\psi_1^2 - \psi_0^2)^2(2\phi - 1) = 0, \quad (3.6)$$

which means that the two phases have the same free energy density. Note that the quadratic term ($\propto \phi^2$) in $\langle f \rangle$ in Eq.(3.3) is positive for $\psi_1 - \psi_0 > 0$. Thus, for small $f_0(\psi_1) - f_0(\psi_0)$, a minimum of $\langle f \rangle$ can be attained as a function of ϕ in the range $[0, 1]$. These equations may be solved for the simple free energy density (2.2). By eliminating ϕ we derive the equations for ψ_1 and ψ_0 as

$$h/v = \psi_1\psi_0(\psi_0 + \psi_1)^3/3, \quad (3.7)$$

$$-u/v = \psi_1^2 + \psi_0^2 + \frac{1}{3}(\psi_0 + \psi_1)^2 \quad (3.8)$$

where u is defined by Eq.(3.1). The negativity of u is required by Eq.(3.8). Thus ψ_1 and ψ_0 are independent of τ . As $h \rightarrow 0$, we have $\psi_0 = 0$ and $\psi_1 = M$, where

$$M = (3|u|/4v)^{1/2}. \quad (3.9)$$

It is convenient to express ψ_1 and ψ_0 as

$$\psi_1 = \frac{q}{2} + \sqrt{\frac{q^2}{4} - \frac{3h}{vq^3}}, \quad \psi_0 = \frac{q}{2} - \sqrt{\frac{q^2}{4} - \frac{3h}{vq^3}}, \quad (3.10)$$

where q satisfies

$$h = \frac{2v}{9}q^3(q^2 - M^2). \quad (3.11)$$

Then q/M is a dimensionless function of h/vM^5 , tending to unity as $h \rightarrow 0$. The difference $\psi_1 - \psi_0 = (q^2 - 12h/vq^3)^{1/2}$ decreases with increasing h . A field-induced criticality is attained for $h = h_c$ and $\tau = \tau_c$, where

$$h_c = (8/5)^{5/2}vM^5/12, \quad (3.12)$$

$$\tau_c = 4vM^4/5 - 2\beta M^2/5. \quad (3.13)$$

The critical value of the order parameter is

$$\psi_c = (2/5)^{1/2}M = (3|u|/10v)^{1/2}. \quad (3.14)$$

For small positive $h_c - h$ we obtain

$$\psi_1 - \psi_0 \cong \frac{2}{5}M(1 - h/h_c)^{1/2}. \quad (3.15)$$

For $h > h_c$ we have a unique one phase state where ψ is determined by Eq.(2.24). In Fig. 2, we show ψ_1/M and ψ_0/M versus h/h_c .

Next the volume fraction of the more ordered phase ϕ is calculated. From Eq.(3.5) it depends on τ as

$$\phi = (\tau_{cx} - \tau)/\tau_w. \quad (3.16)$$

This relation holds for $\beta > \bar{u}$ and $h < h_c$ with

$$\tau_{cx} = -\bar{u}\psi_0^2 - v\psi_0^4 + \frac{v}{3}\psi_1(\psi_0 + \psi_1)^3, \quad (3.17)$$

$$\tau_w = \beta(\psi_1^2 - \psi_0^2). \quad (3.18)$$

In Fig. 2, the normalized window width $\tau_w/\beta M^2$ is also displayed as a function of h/h_c . Since ϕ is in the range $0 < \phi < 1$, the two-phase coexistence is realized in the window region,

$$\tau_{cx} - \tau_w < \tau < \tau_{cx}. \quad (3.19)$$

For τ below τ_{cx} the more ordered phase starts to appear, and τ_w is the width of the temperature window. As $h \rightarrow 0$, τ_{cx} and τ_w tend to the following values,

$$\lim_{h \rightarrow 0} \tau_{cx} = vM^4/3 = 3u^2/16v, \quad (3.20)$$

$$\lim_{h \rightarrow 0} \tau_w = \beta M^2 = 3\beta(\beta - \bar{u})/4v. \quad (3.21)$$

On the other hand, as $h \rightarrow h_c$, the upper and lower bounds in Eq.(3.19) meet at $\tau = \tau_c$ and behave as $\tau_{cx} \cong \tau_c + \beta\psi_c(\psi_1 - \psi_0)$ and $\tau_{cx} - \tau_w \cong \tau_c - \beta\psi_c(\psi_1 - \psi_0)$, where $\psi_1 - \psi_0$ depends on $h_c - h$ as in Eq. (3.15). In Fig. 3, we show the phase diagrams in the τ - h plane for $\bar{u} > 0$ and for $\bar{u} < 0$, separately, where the coexisting curves, $\tau = \tau_{cx}$ and $\tau = \tau_{cx} - \tau_w$, and the instability curves are displayed. The latter are obtained by setting $C\kappa^2 = 0$ in Eq.(2.22) using ψ determined by Eq.(2.19) (see the discussions above Eq.(2.23)). These curves meet at the corresponding critical point $h = h_c$ and $\tau = \tau_c$ given by Eqs.(3.12) and (3.13).

The usual theory of tricriticality^{1,17,18} starts with the free energy density,

$$f = \frac{\tau}{2}\psi^2 + \frac{u}{4}\psi^4 + \frac{v}{6}\psi^6 - h\psi, \quad (3.22)$$

for systems with short-range interactions. For this model a first order phase transition line¹⁹ appears in the τ - h plane for $u < 0$. (i) The line starts from the τ axis ($h = 0$) at the transition point given by $\tau = 3u^2/16v$ where $\psi^2 = 3|u|/4v$ in the emerging ordered phase. These values coincide with those in Eqs.(3.20) and (3.9) in our elastic model. (ii) The line ends at a field-induced critical point, where $\psi^2 = 3|u|/10v$, $h = 8v(3|u|/10v)^{5/2}/3$, and $\tau = 9u^2/20v$. The critical values of ψ and h coincide with those in Eqs.(3.14) and (3.12). However, the critical value of τ is higher than that in Eq.(3.13) by $2\beta M^2/5$.

B. Magnetization, susceptibility, and specific heat

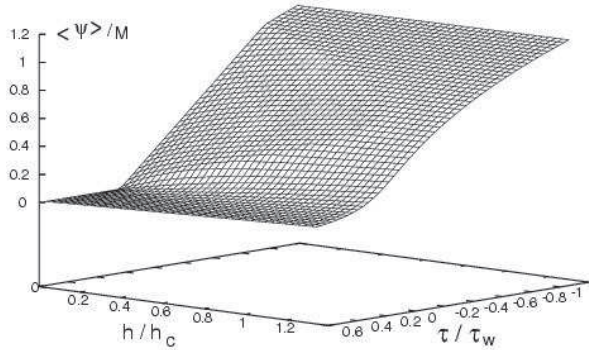


FIG. 4: Normalized average magnetization $\langle \psi \rangle / M$ as a function of h/h_c and τ/τ_w for $\beta/\bar{u} = 1.2$ calculated from Eqs.(2.19) and (3.23), where M , h_c , and τ_w are defined by Eqs.(3.9), (3.12), and (3.18), respectively.

In the two phase states in the temperature window, the average order parameter is given by²⁰

$$\langle \psi \rangle = \phi\psi_1 + (1 - \phi)\psi_0, \quad (3.23)$$

which is continuously connected to the solution of Eq.(2.22) in the one phase states outside the window

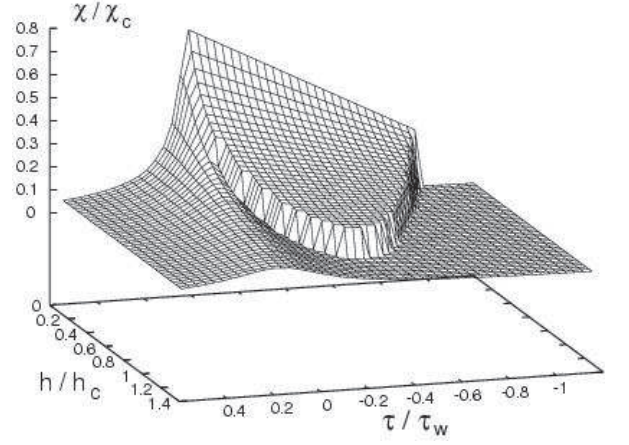


FIG. 5: Normalized susceptibility χ/χ_c as a function of h/h_c and τ/τ_w for $\beta/\bar{u} = 1.2$, where $\chi_c = M/h_c$. It is calculated from Eqs.(2.20) and (3.24). It increases discontinuously at the phase boundary from the one phase region to the two phase region.

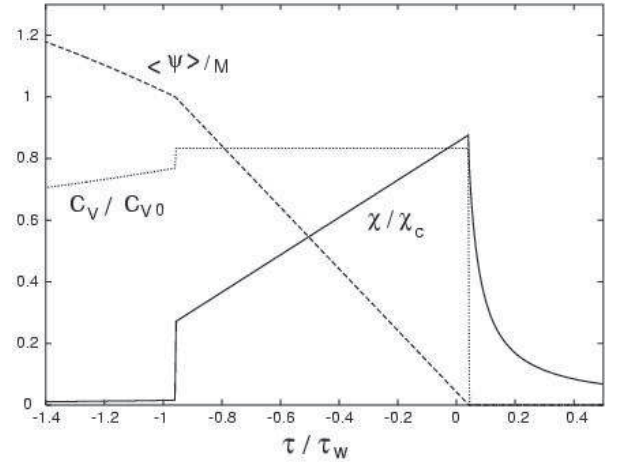


FIG. 6: Normalized average order parameter $\langle \psi \rangle / M$, normalized susceptibility χ/χ_c , and normalized specific heat C_V/C_{V0} versus τ/τ_w for $\beta/\bar{u} = 1.2$ in the limit $h \rightarrow 0$, where $C_{V0} = TA_0^2/2\bar{u}$.

region. See Fig. 4 for $\langle \psi \rangle$ as a function of τ and h at $\beta/\bar{u} = 1.2$. The effective isothermal susceptibility $\chi = (\partial \langle \psi \rangle / \partial h)_\tau$ is calculated from

$$\chi = (\psi_1 - \psi_0) \frac{\partial \phi}{\partial h} + \phi \frac{\partial \psi_1}{\partial h} + (1 - \phi) \frac{\partial \psi_0}{\partial h}, \quad (3.24)$$

where the derivatives are performed at fixed τ . See Fig. 5 for χ as a function of τ and h at $\beta/\bar{u} = 1.2$. We can see that χ is discontinuous at the boundary of the window region. There is no critical divergence in χ at the field-induced criticality attained. In particular, as $h \rightarrow 0$, it behaves as

$$\chi = (1 - 3\phi/4 + 2vM^2/3\beta)/(vM^4/3), \quad (3.25)$$

where $vM^4/3$ is the value of τ_{cx} as $h \rightarrow 0$. For $\tau > \tau_{cx}$ we have $\chi = 1/\tau$ at $h = 0$. Figure 6 displays the behavior of χ on the axis in the limit $h \rightarrow 0$.

Next we consider the specific heat at constant volume $C_V = -T\partial^2\langle f \rangle/\partial T^2$ (per unit volume) arising from the spin degrees of freedom, where h is fixed. In the two phase coexistence with $h < h_c$, we use Eqs.(3.3) and (3.16) to obtain

$$C_V = TA_0^2/2\beta, \quad (3.26)$$

which is independent of h even for $h > 0$. In the one phase region, we have $C_V = TA_0^2\psi^2/(\tau + 3\bar{u}\psi^2 + 5v\psi^4)$, where ψ is determined by Eq.(2.19). In particular, at $h = 0$, $C_V = 0$ for $\tau > \tau_{cx}$ and $C_V = TA_0^2/2\sqrt{\bar{u}^2 - 4v\tau}$ for $\tau < \tau_{cx} - \tau_w$. In Fig. 6, we show C_V versus τ at $h = 0$.

C. Correlation length and surface tension

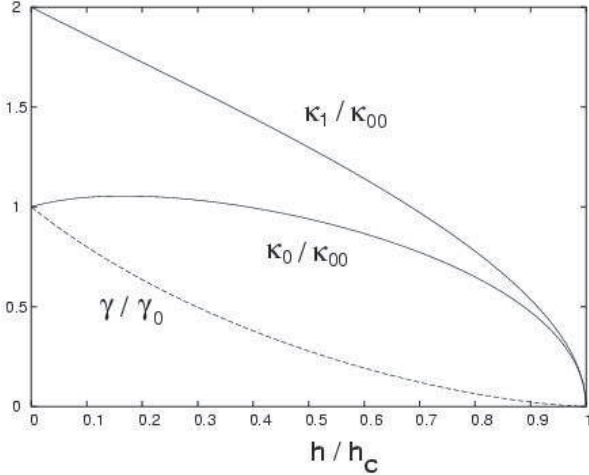


FIG. 7: Inverse correlation lengths κ_0 and κ_1 versus h/h_c in the coexisting two phases. They are divided by κ_{00} in Eq.(3.29). Normalized surface tension γ/γ_0 is also shown, where γ_0 is in Eq.(3.36).

Starting with the first line of Eq.(2.27), we may calculate the inverse correlation lengths, κ_0 and κ_1 , in the coexisting two phases with $\psi = \psi_0$ and ψ_1 , respectively. With the aid of Eqs.(3.6)-(3.8) some calculations yield

$$\kappa_0^2 = \frac{v}{3C}(\psi_1 - \psi_0)^2(\psi_1 + \psi_0)(\psi_1 + 4\psi_0), \quad (3.27)$$

$$\kappa_1^2 = \frac{v}{3C}(\psi_1 - \psi_0)^2(\psi_1 + \psi_0)(4\psi_1 + \psi_0). \quad (3.28)$$

As $h \rightarrow 0$, we have $\kappa_0 \rightarrow \kappa_{00}$ and $\kappa_1 \rightarrow 2\kappa_{00}$, where

$$\kappa_{00} = (v/3C)^{1/2}M^2 \quad (3.29)$$

is the inverse correlation length in the disordered phase at $\tau = vM^4/3$ and $h = 0$. As $h \rightarrow h_c$, the inverse

correlation lengths go to zero as

$$\kappa_0 \cong \kappa_1 \cong (4/5)\kappa_{00}(1 - h/h_c)^{1/2}, \quad (3.30)$$

from Eq.(3.15). If the scattering amplitude is proportional to S_k in Eq.(2.21), it grows near the critical point at long wavelengths. In Fig. 7, we plot κ_0/κ_{00} and κ_1/κ_{00} versus h/h_c . It is worth noting that the inverse correlation length κ in the one phase region also goes to zero at the criticality. In its vicinity, the relations (2.19) and (2.22) in the one phase case give

$$C\kappa^2 \cong (h - h_c)/\psi_c, \quad (3.31)$$

where the term linear in $\tau - \tau_c$ vanishes.

We also calculate the surface tension γ in the two phase coexistence. We suppose a one-dimensional interface profile $\psi = \psi(x)$ changing along the x direction. It changes from ψ_0 at $x = -\infty$ and to ψ_1 at $x = \infty$. From $\delta F/\delta\psi = 0$, we obtain

$$C\frac{d^2\psi}{dx^2} = f'_0(\psi) - \beta(\psi^2 - \langle\psi^2\rangle)\psi. \quad (3.32)$$

We integrate the above equation as $2\omega = C(d\psi/dx)^2$, where $\omega(\psi)$ is the grand potential,

$$\omega = f_0(\psi) - \frac{\beta}{4}(\psi^2 - \langle\psi^2\rangle)^2 - C_0. \quad (3.33)$$

From Eq.(3.6) the constant C_0 in the right hand side can be chosen such that ω vanishes at $x = \pm\infty$ or for both $\psi = \psi_0$ and ψ_1 . Some calculations yield¹

$$\omega = \frac{v}{3}(\psi - \psi_0)^2(\psi - \psi_1)^2[(\psi + \psi_0 + \psi_1)^2 + \psi_0\psi_1], \quad (3.34)$$

which turns out to be independent of τ . The surface tension γ is a function of h only. It is of the form,

$$\begin{aligned} \gamma &= \int_{-\infty}^{\infty} dx[\omega + C(d\psi/dx)^2/2] \\ &= \int_{\psi_0}^{\psi_1} d\psi\sqrt{2C\omega(\psi)}. \end{aligned} \quad (3.35)$$

In the limit $h \rightarrow 0$ it becomes

$$\gamma_0 = \lim_{h \rightarrow 0} \gamma = (vC/24)^{1/2}M^4. \quad (3.36)$$

On the other hand, as $h \rightarrow h_c$, ω in (3.35) behaves as $\omega \cong |u|(\psi - \psi_0)^2(\psi - \psi_1)^2/2$ so that

$$\gamma/\gamma_0 \cong (32/375)(1 - h/h_c)^{3/2}, \quad (3.37)$$

which rapidly decreases near the criticality. See Fig. 7, where γ/γ_0 is plotted.

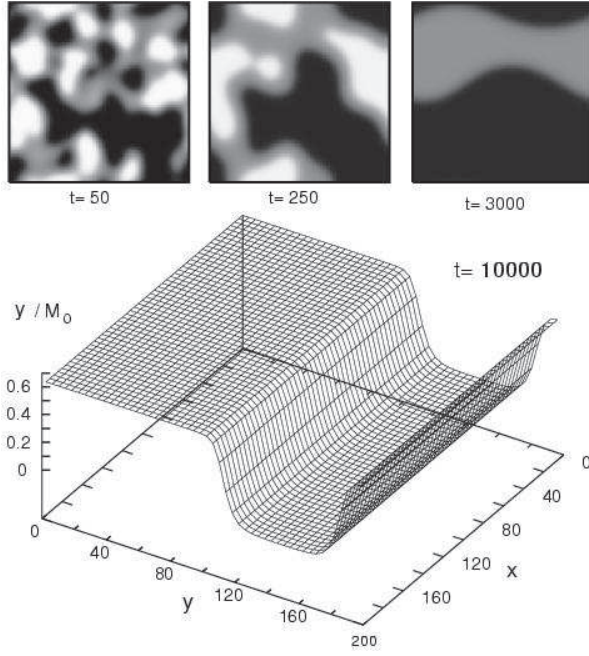


FIG. 8: Time evolution of ψ after changing τ from 0 to $-0.3\tau_0$ at $t = 0$ (upper panel) and steady profile of ψ/M_0 obtained at $t = 10^4$ (lower panel) for $\beta/\bar{u} = 1.5$ and $h = 0$ in isotropic elasticity. Here M_0 is in Eq.(4.2) and space and time are measured in units of ℓ and t_0 in Eq.(4.3). In the initial stage three regions with $\psi \cong \psi_1$ (black), $\psi \cong -\psi_1$ (white), and $\psi \cong 0$ (gray) emerged, but in the final stage $t \gtrsim 10^3$ the variant with $\psi \cong -\psi_1$ disappeared here.

IV. NUMERICAL RESULTS

We numerically study the dynamics of our model. We may demonstrate the validity of our equilibrium theory in steady states attained at long times. In our system ψ is a nonconserved variable obeying the relaxation equation,

$$\frac{\partial}{\partial t}\psi = -L_0 \frac{\delta F}{\delta \psi}, \quad (4.1)$$

where $\delta F/\delta \psi$ is given in Eq.(2.14) and L_0 is a constant. We integrated the above equation in 2D under the periodic boundary condition. We assume $\bar{u} > 0$ and $\beta/\bar{u} = 1.5$. Then, for $h = 0$, our theory predicts $\psi_1 = 0.612M_0$, $\psi_0 = 0$, $\tau_{cx}/\tau_0 = 0.047$, $(\tau_{cx} - \tau_w)/\tau_0 = -0.516$, $\kappa_0\ell = 0.354$, and $\kappa_1\ell = 0.596$.@ These values will be compared with those from our simulations.

A. Isotropic elasticity

We first assume the isotropic elasticity. We measure τ , h , and ψ in units of τ_0 , h_0 , and M_0 , respectively, where

$$\tau_0 = \bar{u}^2/v, \quad h_0 = v(\bar{u}/v)^{5/2}, \quad M_0 = (\bar{u}/v)^{1/2}. \quad (4.2)$$

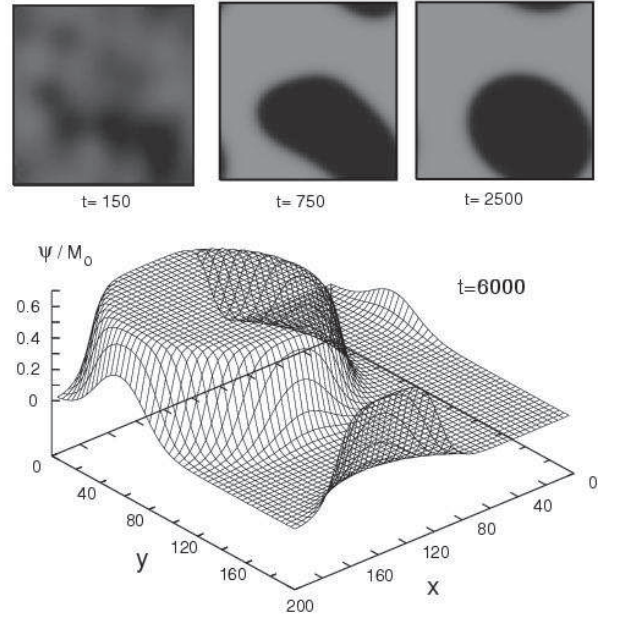


FIG. 9: Time evolution of ψ after changing τ from $-\tau_0$ to $-0.15\tau_0$ at $t = 0$ (upper panel) and steady profile of ψ/M_0 obtained at $t = 6 \times 10^3$ (lower panel) for $\beta/\bar{u} = 1.5$ and $h = 0$ in isotropic elasticity. In the phase ordering, ordered regions with $\psi \cong \psi_1$ (black) and disordered regions (gray) emerged. A circular ordered domain remained at long times in this run.

Here $M/M_0 = [3(\beta/\bar{u} - 1)/4]^{1/2}$ from Eq.(3.9). Units of space and time are

$$t_0 = L_0\tau_0, \quad \ell = (C/\tau_0)^{1/2}. \quad (4.3)$$

The scaled time $t_0^{-1}t$ and the scaled space position $\ell^{-1}\mathbf{r}$ are simply written as t and \mathbf{r} to avoid cumbersome notation. The system size is 200×200 and the mesh length is ℓ , so the system length is 200ℓ . In terms of the scaled order parameter $\Psi = \psi/M_0$, Eq.(4.1) is rewritten as

$$\frac{\partial \Psi}{\partial t} = \left[\nabla^2 - \frac{\tau}{\tau_0} - \Psi^2 - \Psi^4 + \frac{\beta}{\bar{u}}(\Psi^2 - \langle \Psi^2 \rangle) \right] \Psi + \frac{h}{h_0}. \quad (4.4)$$

As the initial condition at $t = 0$, Ψ at each lattice point consists of a homogeneous constant and a random number in the range $[-0.01, 0.01]$.

In Fig. 8, we show the phase ordering process from a disordered state to a coexisting state. At $t = 0$, Ψ was a random number. For $t > 0$ we lowered τ from 0 to $-0.3\tau_0$ to induce phase ordering. From our theory, this final τ is in the coexisting window $[\tau_{cx} - \tau_w, \tau_{cx}]$ and the predicted average order parameter is $0.378M_0$ with $\phi = 0.617$. Since $h = 0$ and $\langle \psi \rangle = 0$ at $t = 0$, the two variants with $\psi = \pm\psi_1$ appeared in the early stage, but the ordered domains with $\psi \cong -\psi_1$ disappeared in this run when the domain size became of the order of the system size. (In other runs the variant with $\psi \cong \psi_1$ disappeared as well.) In the steady two phase coexistence at $t = 10^4$ (lower panel in Fig. 8) interfaces are horizontal (parallel to the x axis), where $\psi = 0.612M_0$ in the

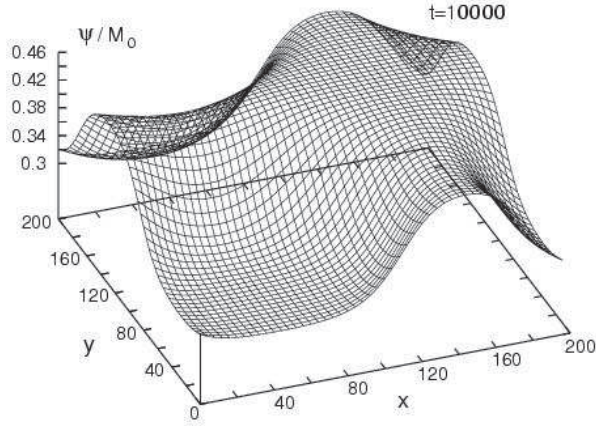


FIG. 10: Steady profile of ψ/M_0 in two phase coexistence obtained at $t = 10^4$ in isotropic elasticity, where $\beta/\bar{u} = 1.5$, $\tau = -0.13\tau_0$, and $h = 0.9h_c$. Here the system is close to the field-induced critical point and the interface region is broadened.

ordered phase and $\langle\psi\rangle = 0.397M_0$. The former coincides with the predicted value, while the latter is slightly larger than predicted.

In Fig. 9, we show the phase ordering process from a one phase state at $\tau = -\tau_0$ to a coexisting state at $\tau = -0.15\tau_0$ at $h = 0$. That is, at $t = 0$, Ψ was the sum of the equilibrium one phase value 0.786 determined by Eq.(2.24) and a random number. The final τ here is higher than the lower instability value $-0.313\tau_0$ in Eq.(2.23). Hence phase ordering should take place into a coexisting state where $\phi = 0.350M_0$ and $\langle\psi\rangle = 0.214M_0$ are predicted. In the simulation, regions of the disordered phase appeared, while ψ in the ordered phase changed to $\psi \cong \psi_1$. In the steady two phase coexistence at $t = 6 \times 10^3$ (lower panel in Fig. 9), a circular ordered domain was realized. There, we find $\psi = 0.594M_0$ in the domain and $\langle\psi\rangle = 0.232M_0$. These values are only slightly different from those predicted.

In Fig. 10, we present a steady profile of ψ at $h = 0.9h_c$ and $\tau = -0.13\tau_0$, where the system is close to the critical point in Eqs.(3.12)-(3.14) and the interface thickness is much widened. For $\beta/\bar{u} = 1.5$ and at this field, our theory gives $\psi_1/M_0 = 0.461$, $\psi_0/M_0 = 0.304$, $\tau_{cx}/\tau_0 = -0.032$, $(\tau_{cx} - \tau_w)/\tau_0 = -0.212$, $\kappa_0\ell = 0.149$, and $\kappa_1\ell = 0.164$. For the τ adopted, we predict $\phi = 0.543$ and $\langle\psi\rangle = 0.389M_0$. In the simulation, the maximum and the minimum of ψ are $0.457M_0$ and $0.302M_0$, respectively. These values are very close to the theoretical values of ψ_1 and ψ_0 . Furthermore, the observed average $\langle\psi\rangle = 0.392M_0$ is also close to its theoretical average, though the interface regions are very wide here.

B. Cubic elasticity

Next we integrate Eq.(4.1) in 2D on a cell of 256×256 assuming the cubic elasticity with $C_{11} - C_{12} = C_{44} = K$,

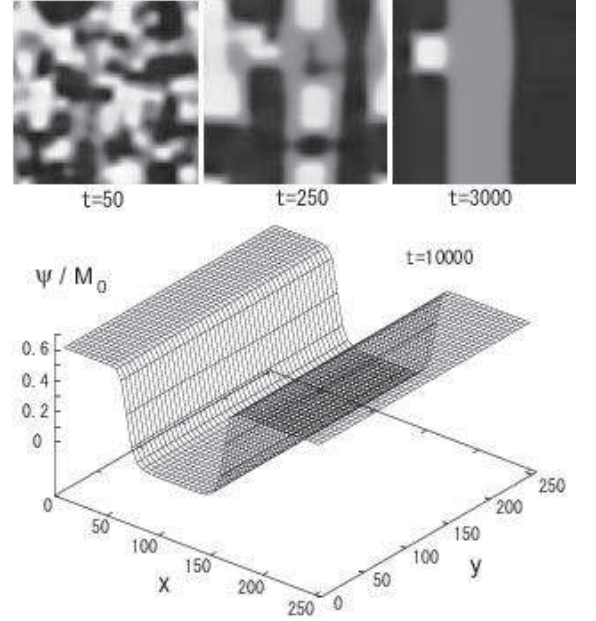


FIG. 11: Time evolution of ψ after changing τ from 0 to $-0.3\tau_0$ at $t = 0$ (upper panel) and final steady profile of ψ/M_0 obtained at $t = 10^4$ (lower panel) in cubic elasticity for $\beta/\bar{u} = 1.5$ and $h = 0$. As in Fig.8, three regions with $\psi \cong \psi_1$ (black), $\psi \cong -\psi_1$ (white), and $\psi \cong 0$ (gray) emerged in the initial stage. Interfaces tend to be parallel to the x or y axis.

where $K = (C_{11} + C_{12})/2$. Then $\xi_a = -1$ from Eq.(2.11) and the softest directions are $[10]$ and $[01]$. As in the isotropic case, space and time are measured in units of ℓ and t_0 in Eq.(4.3) and we set $\beta = 2\alpha^2/C_{11} = 1.5\bar{u} > 0$. The mesh size of integration is ℓ . In terms of the scaled order parameter $\Psi = \psi/\psi_0$, the dynamic equation in the 2D cubic case is written as^{1,13,15,16}

$$\frac{\partial \Psi}{\partial t} = \left[\nabla^2 - \frac{\tau}{\tau_0} - \Psi^2 - \Psi^4 + \frac{\beta}{\bar{u}} G \right] \Psi + \frac{h}{h_0}. \quad (4.5)$$

From Eqs.(2.8) and (2.14) we express $G(\mathbf{r})$ in the Fourier expansion,

$$G(\mathbf{r}) = \frac{1}{w(0)} \sum_{\mathbf{k}} w(\theta) \Phi_{\mathbf{k}} e^{i\mathbf{k} \cdot \mathbf{r}}, \quad (4.6)$$

where $\Phi_{\mathbf{k}}$ is the Fourier component of $\Phi = \Psi^2 - \langle\Psi^2\rangle$ and $w(\mathbf{k}) = w(\theta)$ in Eq.(2.13) depends on the angle θ defined by $\cos \theta = k_x/k$.

In Fig. 11, we lowered τ from 0 to $-0.3\tau_0$ at $h = 0$ as in Fig. 8. Here the anisotropy of the domain structure arises from the angle dependence of $w(\theta)$ in Eq.(4.6). In the steady state in the lower panel, the maximum of ψ is $0.613M_0$ and the average $\langle\psi\rangle$ is $0.393M_0$, in close agreement with the predicted values and those in Fig. 8.

In Fig. 12, we show a steady profile of ψ for $\tau = -0.13\tau_0$ and $h = 0$ as in Fig. 9. Here a square ordered domain is embedded in a disordered region in equilibrium. In the figure, the maximum and the average of ψ

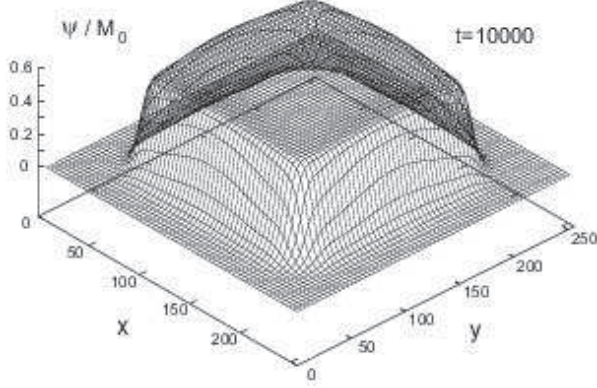


FIG. 12: Steady square profile of ψ/M_0 in two phase coexistence obtained at $t = 10^4$ in cubic elasticity, where $\beta/\bar{u} = 1.5$, $\tau = -0.15\tau_0$, and $h = 0$.

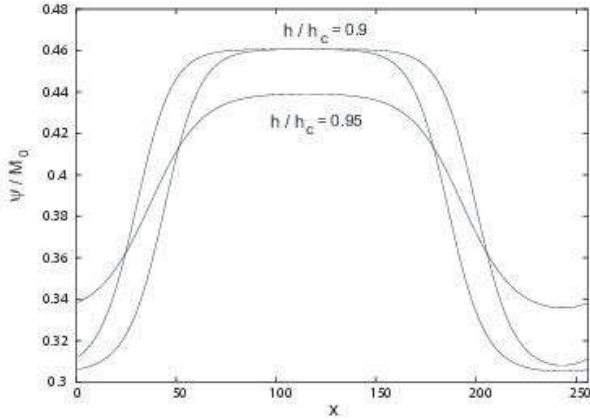


FIG. 13: Steady, one-dimensional curves of ψ/M_0 in two phase coexistence with $\beta/\bar{u} = 1.5$ near the field-induced critical point in cubic elasticity. Here $\tau = -0.13\tau_0$ and $-0.15\tau_0$ for the two curves of $h = 0.9h_c$, while $\tau = -0.13\tau_0$ for $h = 0.95h_c$. The more ordered region expands with lowering τ at fixed h .

are $0.586M_0$ and $0.260M_0$, respectively. The former is slightly smaller than the predicted value $0.612M_0$, while the latter is considerably larger than the predicted value $0.214M_0$.

In Fig. 13, we show one-dimensional steady profiles changing along the x axis near the critical point. The maximum, the minimum, and the average of ψ are $(0.461, 0.305, 0.392)$ for $h/h_c = 0.9$ and $\tau/\tau_0 = -0.13$, $(0.461, 0.308, 0.409)$ for $h/h_c = 0.9$ and $\tau/\tau_0 = -0.15$, and $(0.439, 0.336, 0.398)$ for $h/h_c = 0.95$ and $\tau/\tau_0 = -0.13$. These values closely agree with those from our theory. In these one-dimensional cases, the profiles coincide with those in the isotropic case.

V. SUMMARY AND CONCLUDING REMARKS

We have examined the phase transition behavior of compressible Ising models at fixed volume in the mean

field theory. In our model the order parameter ψ is isotropically coupled to the dilation strain e_1 as $\psi^2 e_1$ in the free energy, which is the simplest case. Nevertheless, complicated phase behavior follows at constant volume. We summarize our main results.

(i) We have found two phase coexistence in a closed region in the τ - h plane as in Fig. 3. The coexistence region appears under the condition $\bar{u} < \beta$ given in Eq.(3.1). If $\bar{u} > 0$ and β is not large, it can be satisfied near the tricritical point. If $\bar{u} < 0$, it can occur even away from the tricritical point.

(ii) The order parameter values in the two phases, ψ_1 and ψ_0 , are determined by h only and is independent of τ as in Fig. 2. The average order parameter $\langle\psi\rangle = \phi\psi_1 + (1-\phi)\psi_0$ is increased smoothly as τ is decreased in the window region $\tau_{cx} - \tau_w < \tau < \tau_{cx}$ for $h < h_c$, since the volume fraction ϕ depends on τ as in Eq.(3.16). The average order parameter $\langle\psi\rangle$ and the susceptibility $\chi = \partial\langle\psi\rangle/\partial h$ are displayed in Figs. 4-6. The specific heat C_V is a constant in two phase coexistence as in Eq.(3.26).

(iii) At the field-induced critical point $h = h_c$ and $\tau = \tau_c$, the correlation length $1/\kappa$ grow and the surface tension γ goes to zero as in Fig. 7, while χ does not diverge.

(iv) We have integrated the dynamic equation, which is Eq.(4.4) for the isotropic elasticity and Eq.(4.5) for the cubic elasticity. A change of τ from the one phase region into the unstable region induces phase ordering as illustrated in Figs. 8-13. It can occur with decreasing τ as in Figs. 8 and 11 and with increasing τ as in Fig. 9. In the final two phase states, the values of ψ and its space average closely agree with the theoretical values.

We make some further remarks.

(i) At constant pressure, two phase coexistence occurs only on a line in the τ - h plane as in the rigid lattice case, but phase separation can be much affected by the elastic coupling (see the appendix)²¹. It is worth noting that the transition depends on the sample shape in hydrogen-metal systems at constant pressure^{1,22}, where the proton concentration is linearly coupled to the dilation¹³.

(ii) We mention Monte Carlo simulations on a binary alloy by Landau's group^{10,11,12}. They assumed that a mixture undergoing unmixing corresponds to ferromagnets and that forming a superstructure to antiferromagnets. In these cases, different results followed in the fixed volume and fixed pressure conditions. However, the unmixing transition in the presence of the size difference¹ is not isomorphic to the ferromagnetic transition. In the former the linear coupling¹³ appears between the concentration c and e_1 in the form ψe_1 , while in the latter the exchange interaction does not break the invariance of $\psi \rightarrow -\psi$ and the elastic coupling is quadratic as $\psi^2 e_1$. At present we cannot compare our theory and their simulations.

(iii) Yamada and Takakura numerically solved a time-dependent Ginzburg-Landau model for an order parameter and a strain in one dimension. They found appearance of a disordered region in a lamellar ordered

region²³. Their finding is consistent with our theory.

(iii) In real metamagnets, there is no field conjugate to the antiferromagnetic order and the tricriticality has been realized by changing magnetic field or hydrostatic pressure. At fixed volume, our theory predicts two phase coexistence in a temperature window near the tricritical point and near the line of first order phase transition. From Eq.(3.21) the width of the window sensitively depends on the coupling constant α as $\tau_w/A_0 = 3\beta(\beta - \bar{u})^2/4vA_0$, where A_0 is the coefficient in Eq.(2.3) and $\beta = 2\alpha^2/K$.

(iv) In our mean field theory, we have neglected the renormalization effect near the critical point, which can be intriguing in the presence of the cubic elastic anisotropy^{8,9}. It should be further studied together with the influence of the global elastic constraint studied in this work.

(v) We should generalize our theory to more complex systems. At the ferroelectric transition¹⁸, the polarization vector is coupled to the strains. In binary alloys, phase separation and an order-disorder phase transition can take place simultaneously¹, where the concentration c and the structural order parameter ψ are both coupled to e_1 in the form $(\alpha_1 c + \alpha_2 \psi^2)e_1$ in the free energy²⁴. There can also be a number of anisotropic elastic couplings between the order parameter and the tetragonal or shear strain. We will soon report on phase transition including a Jahn-Teller coupling²⁵.

Acknowledgments

We would like to thank B. Dünweg for informative correspondence. This work was supported by Grants in Aid for Scientific Research and for the 21st Century COE project (Center for Diversity and Universality in Physics) from the Ministry of Education, Culture, Sports, Science and Technology of Japan.

Appendix A: Fixed pressure condition

We here eliminate the elastic field at fixed pressure^{2,4,11}. Under isotropic applied stress, we assume an isotropic average dilation change $\langle e_1 \rangle$ caused by the order parameter change. The average stress should be unchanged from that in the reference state, so we require $\langle \sigma_{ij} \rangle = 0$ in Eq.(2.6) to obtain

$$\langle e_1 \rangle = -\alpha \langle \psi^2 \rangle / K, \quad (\text{A.1})$$

in terms of the bulk modulus K . We impose the periodic boundary condition on the deviation, $\delta u_i = u_i - \langle e_1 \rangle x_i / d$, whose Fourier component can be expressed in terms of $\varphi_{\mathbf{k}}$ in the same form as that of u_i in the fixed volume case. The free energy consists of F in Eq.(2.15) and

$$\Delta F = -V\alpha^2 \langle \psi^2 \rangle^2 / 2K. \quad (\text{A.2})$$

The total free energy $F' = F + \Delta F$ is written as

$$F' = \int d\mathbf{r} \left[f + \frac{C}{2} |\nabla \psi|^2 + \frac{B}{4} (\psi^2 - \langle \psi^2 \rangle)^2 \right], \quad (\text{A.3})$$

where $f = f_0 - \alpha^2 \psi^4 / 2K$ and B is a positive coefficient,

$$B = 2\alpha^2 / K - 2w_M. \quad (\text{A.4})$$

Here w_M is given by Eq.(2.17). The positivity of B arises from $C_{11} - C_{12} > 0$ and $C_{44} > 0$. The one phase ordered states are determined by f . The same form of the free energy was derived by Littlewood and Chandra²¹ for BaTiO₃, who argued that the term proportional to B can much decrease the nucleation rate from the paraelectric to ferroelectric state. In our problem, we draw the following conclusion in the mean field theory. In the fixed pressure condition, there can be two phase coexistence only on a first-order coexistence line in the τ - h plane. In fact, $\langle f \rangle$ in Eq.(3.3) would be minimized for $\phi = 0$ or 1 outside the coexistence curve if positive β were replaced by negative $-B$.

¹ A. Onuki, *Phase Transition Dynamics* (Cambridge University Press, Cambridge, 2002).

² A. I. Larkin and S.A. Pikin, Zh. Exsp. Teor. Phys. **56**, 1664 (1969) [Sov. Phys. JETP **29**, 891 (1969)].

³ G. A. Baker, Jr. and J. W. Essam Phys. Rev. Lett. **24**, 447-449 (1970); G. A. Baker, Jr. and J. W. Essam, J. Chem. Phys. **55**, 861 (1971).

⁴ J. Sak, Phys. Rev. B **10**, 3957 (1974).

⁵ Y. Imry, Phys. Rev. Lett. **33**, 1304 (1974).

⁶ F. Wegner, J. Phys. C **7**, 2109 (1974).

⁷ J. Oitmaa and M. N. Barber, J. Phys. C **8**, 3653 (1975).

⁸ D. J. Bergman and B. I. Halperin, Phys. Rev. B **13**, 2145 (1976).

⁹ M. A. de Moura, T. C. Lubensky, Y. Imry, and A. Aharony, Phys. Rev. B **13**, 2176 (1976).

¹⁰ F. Tavazza, D. P. Landau, and J. Adler, Phys. Rev. B **70**, 184103 (2004)

¹¹ X. Zhu, F. Tavazza, D. P. Landau, and B. Dünweg, Phys. Rev. B **72**, 104102 (2005).

¹² D. P. Landau, Brazilian Journal of Physics, **36**, 640 (2006).

¹³ In binary mixtures^{15,16}, the concentration c is coupled in the form $\alpha c e_1$ in the free energy density when the atomic sizes of the two components are different¹. There, $\varphi_{\mathbf{k}}$ in Eqs.(2.8) and (2.12) is replaced by the Fourier component $c_{\mathbf{k}}$ of the concentration. The concentration dependence of the elastic moduli is relevant here, leading to a first order phase transition into a glassy ordered state¹.

¹⁴ A. G. Khachatryan, *Theory of Structural Transformations in Solids*, (John Wiley & Sons, New York, 1983).

¹⁵ H. Nishimori and A. Onuki, Phys. Rev. B **42**, 980 (1990).

- ¹⁶ P. Nielaba, P. Fratzl, and J. L. Lebowitz, J. Stat. Phys. **95**, 23 (1999).
- ¹⁷ R.B. Griffiths, Phys. Rev. B **7**, 549 (1973).
- ¹⁸ E. Courtens and R.W. Gammon, Phys. Rev. B **24**, 3890 (1981).
- ¹⁹ For the free energy density (3.22) the first order phase transition line is expressed as $\tau = v(4M^4 - 6M^2q^2 + 5q^4)/9$ in terms of $q = \psi_1 + \psi_0$, where q is related to h by Eq.(3.11) and $\psi_1 - \psi_0 = [(8M^2 - 5q^2)/3]^{1/2}$.
- ²⁰ At $h = 0$, the two variants with $\psi = \pm\psi_1$ may be present in large systems, while only one of them survived in our simulations in Figs. 8 and 11. Thus we assume $h > 0$ in Eq.(3.23) and take the limit $h \rightarrow 0$ in Fig. 6.
- ²¹ P.B. Littlewood and P. Chandra, Phys. Rev. Lett. **57**, 2415 (1986).
- ²² H. Wagner and H. Horner, Adv. Phys. **23**, 587 (1974).
- ²³ Y. Yamada and T. Takakura, J. Phys. Soc. Japan **71**, 2480 (2002).
- ²⁴ C. Sagui, A. M. Somoza and R.C. Desai, Phys. Rev. E **50**, 4865 (1994).
- ²⁵ A. Onuki, J. Phys. Soc. Japan **70**, 3479 (2001).